ABSTRACT

Title of Document: IMPACTS OF INTERMEDIATE WATER FORMATION IN THE NORTH PACIFIC ON INDONESIAN THROUGHFLOW AND EQUATORIAL THERMOCLINE DEPTH: A HIGH LATITUDE CONTROL FOR ENSO VARIABILITY?

Elizabeth Kaye Brabson, Master of Science, 2008

Directed By: Professor James Farquhar
Department of Geology

Long-term variability in the strength and frequency of the El Niño – Southern Oscillation (ENSO) may be attributable to changes in background climatology. During times of cold climate events in the high latitudes, El Niño conditions may have been more persistent in the equatorial Pacific. In this study, a numerical ocean model was used to examine the role oceanic circulation may play in linking these two regions. The simulation of an intermediate body of water of 10 Sv in the North Pacific results in an overall decrease in flow of 29% across the Indonesian Seaways. No change in the overall structure of the thermocline was observed; however the model predicted warming of the surface water in the western and eastern tropical Pacific. It is, therefore hypothesized that a sinking water mass in the North Pacific could have fueled either more permanent El Niño – like conditions or more frequent/intense ENSO events.

IMPACTS OF INTERMEDIATE WATER FORMATION IN THE NORTH PACIFIC ON INDONESIAN THROUGHFLOW AND EQUATORIAL THERMOCLINE DEPTH: A HIGH LATITUDE CONTROL FOR ENSO VARIABILITY?

By

Elizabeth Kaye Brabson

Thesis submitted to the Faculty of the Graduate School of the
University of Maryland, College Park, in partial fulfillment
of the requirements for the degree of
Master of Science
2008

Advisory Committee:
Professor James Farquhar, Chair
Professor Ragu Murtugudde
Professor Roberta Rudnick

Acknowledgements

I would first like to thank my advisors, Dr. Ragu Murtugudde and Dr. James Farquhar for their patience and support during this project. I am also especially grateful to Matthew Harrison from NOAA's Geophysical Fluid Dynamics Laboratory in Princeton, New Jersey, without whom completion of the model simulations on MOM4 would not have been possible. Funding for this project was generously provided by NASA Goddard Space Flight Center through their Earth System Science Fellowship, and also through the financial support from Drs. Murtugudde and Farquhar.

I would like to thank the staff of Geology and ESSIC for the work they do and for the supportive and positive manner in which they complete their job. It is truly a pleasure to deal with each and every one of you.

I would like to thank my family for their unwavering support and encouragement. There is nothing more special in life than having the love and support of people who truly want to see you succeed. I especially want to thank my husband, Tommy, for his unconditional support and encouragement. During the difficult times of the past two years, when I thought it would be impossible to complete this project, he never let me lose sight of my goal. He has helped me to remain positive and has continuously helped to raise my morale. Finally, I would like to thank my beautiful sons, John and Jeffrey, for bringing such joy into my life. Your courage, strength, and passion for life have been a true inspiration.

Table of Contents

List of Figures

Chapter 1: INTRODUCTION

1.1 Overview

The consequences of climate change have become increasingly apparent in recent years. With each decade of research, scientists learn more about the complex interactions impacting climate, yet the system as a whole remains to be fully understood. This is due to the forcings and feedbacks that occur within and between components of the atmosphere, hydrosphere, biosphere, cryosphere, and geosphere. To fully appreciate different modes of variability and the important processes of interest within the climate system, it is first essential to tease apart the influence of each individual component, and then build upon that with a coupled approach.

The Earth's oceans play an important role in determining climate variability mainly due to their ability to store and to transfer heat. Processes affecting the thermal regulation of the oceans can be external or internal to the Earth system. The primary external control is the variability of solar output, which influences the amount of solar radiation received at the top of the Earth's atmosphere. Internal thermal controls are more complex and include elements such as the transfer of heat through surface interactions with the overlying atmosphere, advection, and the global thermohaline circulation. Variations in these mechanisms through time may combine to cause significant changes in the thermal structure of the tropical oceans. The principal mode of modern climate variability, the El Niño-Southern Oscillation (ENSO), originates in the tropical Pacific Ocean. Therefore, changes in the mean climatological state of this region in the past could have impacted the frequency and amplitude of ENSO events.

In this study, a sensitivity test to internal thermal constraints was conducted. Specifically, a numerical ocean model was used to simulate intermediate water formation in the Northern Pacific. The results are examined for impacts to the heat budget of the tropical Pacific Ocean and used to hypothesize about their impact on ENSO variability. The remainder of this Chapter provides a background review. This includes an overview of ENSO and its variability through time, a discussion of the mechanisms influencing the background climatology of the tropical Pacific, a review of the heat budget of the tropical Pacific, and the more specific role of Indonesian throughflow and meridional overturning circulation (MOT) on thermal processes in the tropics. Chapter 2 provides a description of the methodology, including experiment design. Chapter 3 describes the results of the model runs, and Chapter 4 discusses the potential implications of the imposed perturbation on ENSO variability.

1.2 The El Niño – Southern Oscillation

The most dominant signal of climate variability seen today originates in the equatorial Pacific. This signal is known as the El Niño-Southern Oscillation (ENSO) and is named for its two defining components. The Southern Oscillation is the atmospheric component. It is measured as the difference in atmospheric pressure at sea level between Tahiti and Darwin and is reported as the Southern Oscillation Index (SOI) (see Figure 1). The SOI has negative values during warm events and positive

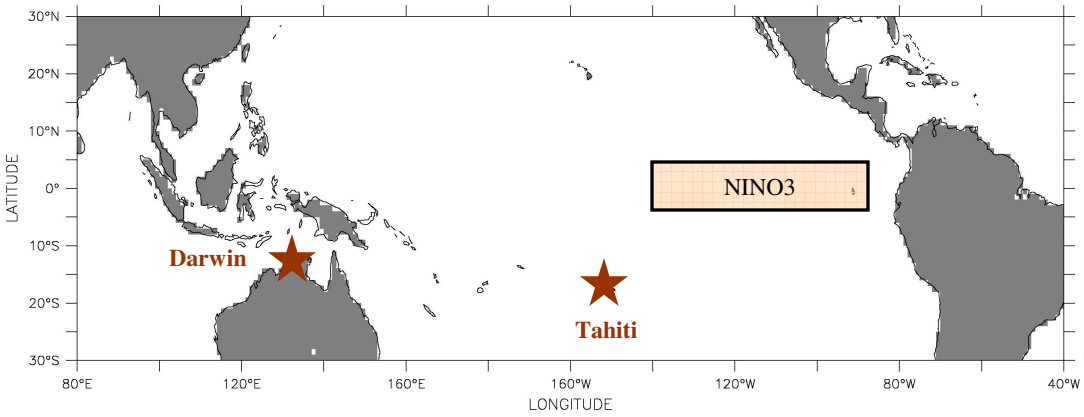

Figure 1. Map illustrating the locations where the atmospheric and oceanic components of ENSO are measured. Differences in atmospheric pressure between Tahiti and Darwin are used to calculate the Southern Oscillation Index. Sea surface temperature anomalies are averaged over the NINO3 region of the central and eastern equatorial Pacific and used as indicators of El Niño and La Niña conditions.

values during cold events. The El Niño component of ENSO is a measure of sea surface temperature (SST) anomalies in the eastern and central equatorial Pacific. Positive SST anomalies in the Niño 3 region are indicative of El Niño, and negative anomalies occur during La Niña (see Figure 1). In the tropics, the atmosphere and the ocean interact in an unstable manner, with an original perturbation growing via positive feedback mechanisms (see e.g., Philander et al. 1984). Bjerknes (1969) was the first to realize these pronounced coupled feedbacks between the thermocline, sea surface temperatures, and the overlying atmosphere in the equatorial oceans, as such; the process is referred to as the Bjerknes Feedback (see Figure 2).

In the modern tropical Pacific, the mean climatology consists of wind-driven upwelling along the western coast of South America, which causes the thermocline to shoal, bringing correspondingly cool water with it to the surface. In contrast, the western equatorial Pacific has a relatively deep thermocline and correspondingly warm surface water (commonly referred to as the western warm pool). In response,

an atmospheric circulation cell forms along the equator, with the deepest atmospheric convection occurring over the western warm pool. The eastern limb of the convective cell occurs over the colder waters of the upwelling region, where the air mass subsides. This zonal atmospheric cell is called Walker Circulation (see Figure 2). Variability associated with ENSO occurs when this delicate balance of sea surface temperature and atmospheric convection is perturbed. During periods when the zonal SST gradient is high, the easterly trade winds and Walker Circulation are enhanced (see Figure 2). The enhanced easterlies promote stronger oceanic upwelling along the western coast of South America, thus fueling a strong Bjerknes feedback. This phase of ENSO is called La Niña or a cold event. During the El Niño phase of ENSO, the zonal sea surface temperature gradient weakens, the reasons for which are not yet fully understood. This triggers a relaxation of the easterly trade winds and the corresponding suppression of the thermocline along the western coast of South America (see Figure 3). Warm water that had built up in the western portion of the basin advects eastward, taking with it the western convective limb of the Walker Cell.

ENSO events have significant impacts on local, regional, and global climate. Shifted patterns of precipitation and marine productivity can have considerable economic and social implications. For these reasons, the study of ENSO dynamics, its driving components, response to background climatology, and patterns of variability are of considerable importance. There is evidence that ENSO has been operating for *at least* the last 130 kyrs (Tudhope et al., 2001), and likely for the last 3 Myrs (e.g., Philander and Fedorov, 2003). In light of future anthropogenic climate change, it may continue to be of considerable importance.

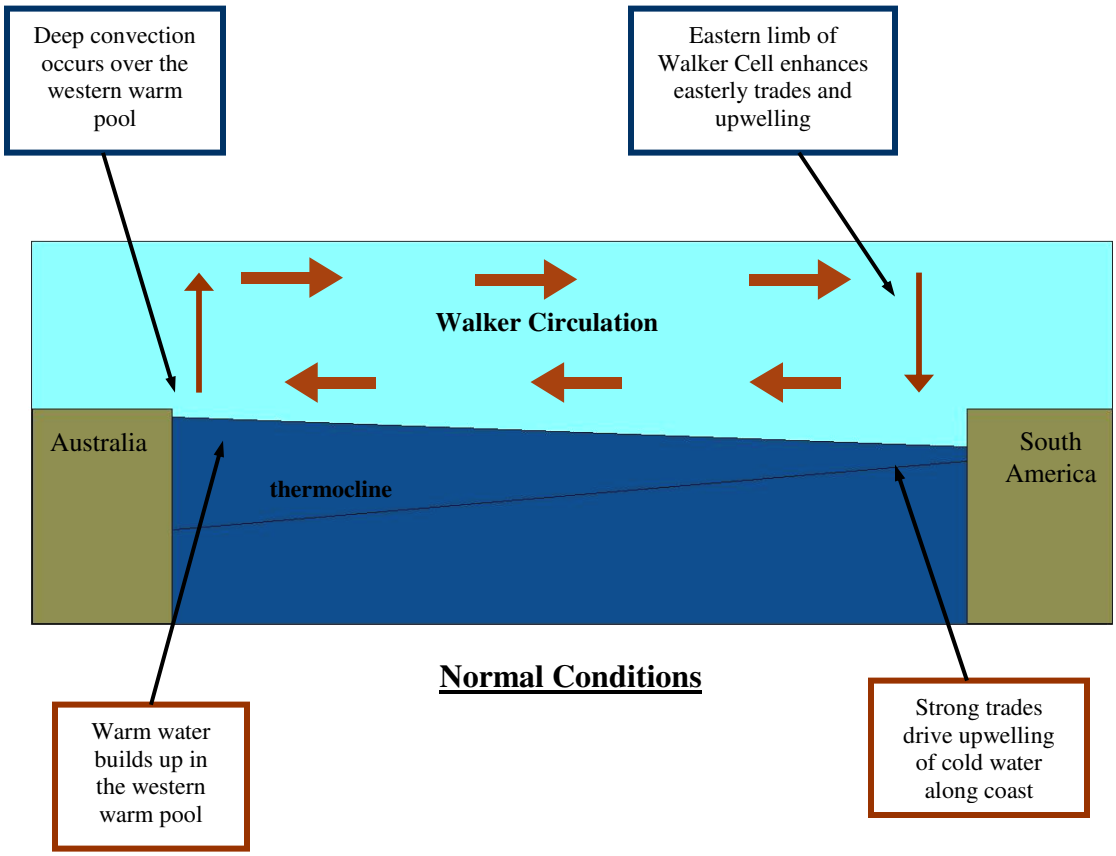

Figure 2. Cartoon illustrating normal climatological conditions across the tropical Pacific Ocean. The thermocline tilts up in the eastern portion of the basin as a result of wind driven upwelling. Warm water advects west, where it accumulates in the western warm pool. A walker circulation cell forms in the atmosphere in response to the underlying sea surface temperatures, with the region of greatest convection occurring over the western warm pool. The subducting eastern limb of the Walker Cell serves to enhance the easterly trades in this region, thus fueling a positive Bjerknes feedback. An amplification of these normal conditions is referred to as a La Niña or cold event, due to the strengthened upwelling of cold water in the eastern Pacific.

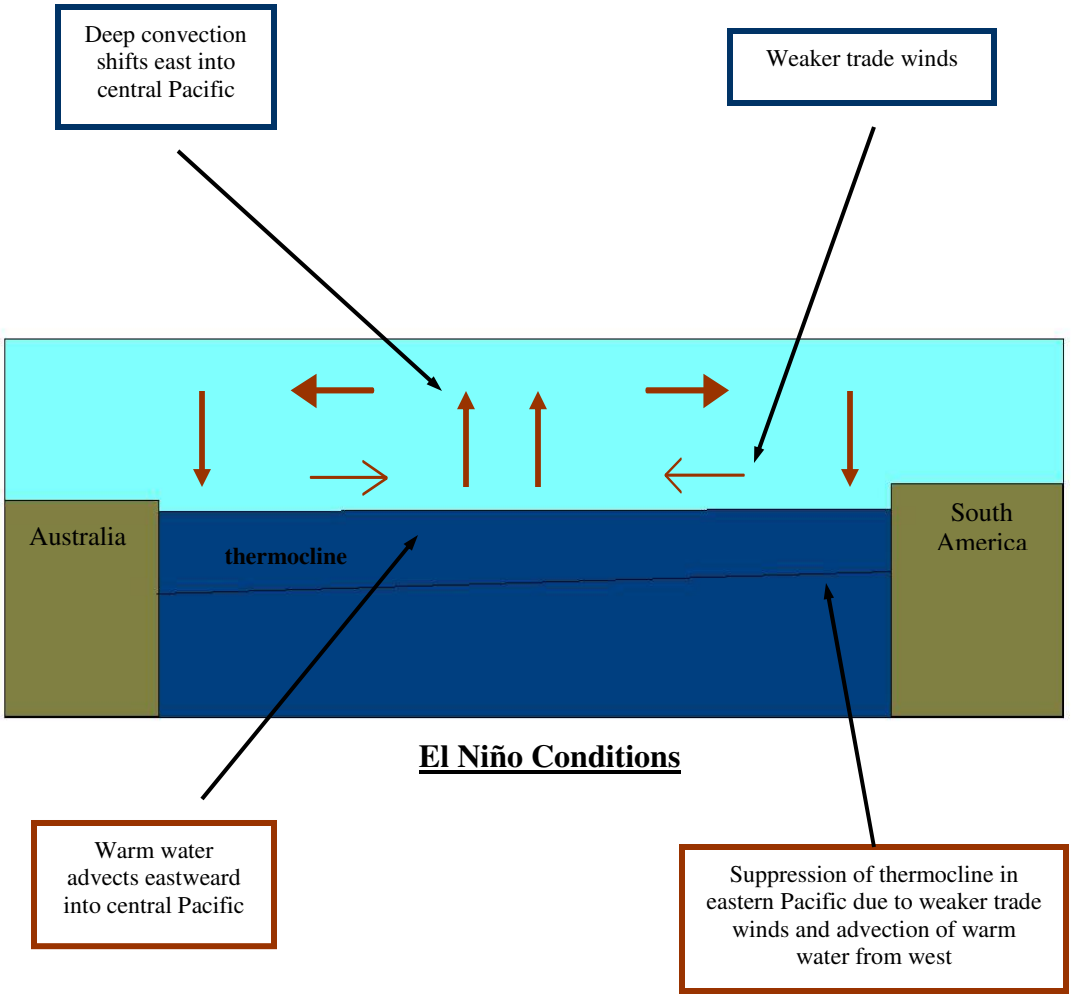

Figure 3. Cartoon illustrating typical El Niño conditions across the tropical Pacific Ocean. A shifting of the western warm pool towards the central portion of the Pacific Basin leads to a corresponding shift in atmospheric convection. This shift in the Walker Cell results in weaker trade winds in the east and suppression of the thermocline due to decreased wind driven upwelling. Warm water from the western Pacific advects eastward, further suppressing the thermocline in the east.

1.2.1 Temporal Variability of the ENSO

The primary mode of ENSO variability is interannual, with warm events occurring roughly every 2 to 7 years. Control of this frequency, or the short-term "memory," is believed to be contained within the ocean basin and transmitted via planetary waves (see e.g., Suarez and Schopf, 1988; Philander, 1990). The development of warm events is tightly locked with the phase of the seasonal cycle (Rasmusson and Carpenter, 1982), and may also be impacted by stochastic elements such as westerly wind bursts (see e.g., Picaut et al., 2002). Our understanding of short-term ENSO variability has greatly improved over the past 30 years due to the availability of diverse sets of data, such as those collected using in situ methods (e.g., McPhaden et al., 1998) and remote satellite methods (e.g., Gurney et al., 1993), and also due to the continuing advances in computer modeling (see e.g., TOGA Special Issue of JGR-Oceans, 1998).

While the dynamical mechanisms driving the termination and interannual nature of warm events are fairly well-documented, other factors, such as background climatology, which can lead to longer-term fluctuations in the strength and frequency of ENSO, are not fully explored. Instrumental records documenting ENSO variability are limited in their temporal coverage. Therefore, researchers collect and analyze paleoproxies, or secondary lines of evidence, which can be used as indicators of past climatic conditions. Of particular interest to this study is the behavior of the ENSO system during times of glacial climatological regimes.

Paleoproxy data suggest that El Niño conditions may have been more permanent or more intense during times of large scale glaciations [e.g. Rodbell et al.,

1999; Stott et al., 2002; Koutavas et al., 2002; Kukla et al., 2002] [see e.g., Lea et al., 2000; Andreasen and Ravelo, 1997 for alternate views]. Stott et al. (2002) use sediment cores and isotopic analyses of planktonic foraminifera to interpret climatic conditions in the western equatorial Pacific during the last 70 kyrs. They found that, when the northern high latitudes were experiencing stadial or cold interglacial conditions, the western equatorial Pacific had an increase in surface salinity and a decrease in precipitation, both indicative of more frequent or severe El Niño events. Conversely, these authors found that during interstadials in the high northern latitudes, the data from the western equatorial Pacific suggest less frequent or less severe El Niño events were occurring. Similarly, Rodbell et al. (1999) analyzed sediment cores from alpine lakes in Ecuador as indicators of ENSO intensity. They found that the periodicity of warm events has shifted in the last 15 kya, with a weaker signal of El Niño periodicity (≥15 years) occurring between 15 and 7 kya, and the transition to the modern periodicity of 2-8.5 years occurring around 5 kya. Data from the Galapagos, in the eastern equatorial Pacific, are also in agreement with more persistent El Niño-like conditions during the last glacial maximum (Koutavas et al., 2002). Likewise, model simulations conducted by Kukla et al. (2002), with imposed solar forcing representative of glacial conditions 111 kya, also corroborate the glacial-strong El Niño link. The observed trends in these data suggest that climatological variations associated with glacials may be a driving mechanism of ENSO variability. The following section provides a review of two potential mechanisms linking background climatology and ENSO.

1.3 Mechanisms of Variability

1.3.1 Solar Variations and the ENSO

Subtle variations in the geometry of Earth's orbit, also referred to as Milankovitch cycles, cause fluctuations in the amount of solar insolation received at the top of the Earth's atmosphere (Milankovitch, 1941). This is believed to have been one of the main drivers of glacial cycles during the last 3 Myrs (see e.g., Hays et al., 1976; Berger, 1979). Each of the three dominant modes of periodicity (precession, obliquity, and eccentricity) influence the Earth's climate differently. The precessional cycle repeats every 23,000 years and has a heavy influence on low latitude seasonal extremes (see e.g., Liu and Herbert, 2004 and references therein). Annual insolation anomalies resulting from the precessional cycle, however, equal zero when averaged over all latitudes. The obliquity cycle is driven by changes in the tilt of the Earth's axis and completes a cycle every 41,000 years. The resulting annual insolation anomalies do not average to zero over all latitudes. During periods of high obliquity, the high latitudes receive more solar insolation and the low latitudes receive less, thereby increasing the seasonality. During periods of low obliquity, the seasonal cycle is damped. The obliquity cycle is often referred to as a polar signal, since the high latitudes are most greatly affected by it. The eccentricity cycle has the longest period of roughly 100,000 years, and it is driven by changes in the elliptical nature of the Earth's orbit.

Elements driving long-term ENSO variability may be directly attributable to Milankovitch forcing. Various model studies have been performed to examine the sensitivity of the ENSO system to solar irradiance (e.g., Clement et al.,1999, 2000;

Kukla et al., 2002). Clement and colleagues performed long simulations using the Zebiak-Cane (CZ) coupled model (Zebiak and Cane, 1987) to test the sensitivity of ENSO variability to the Milankovitch cycles. They found that, in this limited domain model, ENSO responded most strongly to the 23 kyr precessional cycle, and not at all to the 41 kyr obliquity cycle (Clement et al., 1999). A similar study by Kukla et al. (2002), used the CZ model to test ENSO sensitivity to climatic forcing similar to conditions that existed 111 kya, when perihelion occurred in boreal spring and aphelion in boreal autumn, causing increased seasonality. The model results predicted stronger and more intense El Niño conditions in the equatorial Pacific during stadial conditions. This is in agreement with proxy evidence, which suggest a more El Niño-like state during glacials (see Section 1.2.1).

The significance of these long-term orbital patterns becomes increasingly important when one considers their impact on global climate and the potential feedbacks within the system. For example, the obliquity cycle is believed to have become the dominant force driving climate variability around 3 Mya (Philander and Fedorov, 2003). Internal feedbacks between the oceans and atmosphere could have been the method of communicating this polar signal to the global climate (Liu and Herbert, 2004). Meridional temperature contrasts brought about by increased seasonality may be one potential link between the high latitude forcing and lower latitude response at the 41 kyr period.

1.3.2 High Latitude – Low Latitude Links

Philander and Fedorov (2003) examine links between the high and low latitudes for their potential response to solar forcing, and their role in the periodicity of climate change over the past 5 Myrs. They cite paleoproxy data, which provide evidence that the thermocline in the eastern equatorial Pacific only became shallow around 3 Mya, initiating favorable conditions for the unstable interactions between the sea and air that are seen today. This upward shift of the thermocline also corresponded to a shift of climatic conditions in this region, with an increased sensitivity to the 41kyr obliquity cycle, also referred to as the polar signal (see Section 1.3.1). Liu and Herbert (2004) analyzed an ocean core from the eastern equatorial Pacific (EEP), which provided further evidence of an obliquity-dominated climate in the EEP from 0.5 to 1.8 Mya. Philander and Fedorov (2003) contend that this high latitude control on equatorial climate was likely a result of high latitude controls on the global ocean heat budget. Philander and Fedorov propose that this was a time of transition, where the deep oceans were cooling, due to deep water formation at high latitudes. As the deep ocean cooled, the low latitude thermocline would have shoaled, giving rise to the zonal gradient seen today.

Previous model studies of the periodicity of climate in the equatorial Pacific have limitations due to constraints on the model domain (see e.g., Clement et al., 1999, 2000). Other investigations, which incorporate links with the extratropics and high latitudes, are beginning to shed light on the full complexity of the problem (see e.g., Latif and Barnett, 1994; Gu and Philander, 1997; Zhang et al., 1998; Schneider et al., 1999). It is apparent that global feedbacks and responses to background

climatological conditions are of key importance, in particular to describing the oceanic heat budget.

1.4 Background Climatology and the ENSO

1.4.1 The Equatorial Pacific Heat Budget

The thermal structure of the equatorial Pacific Ocean is a key factor in determining climate variability via interannual processes, such as ENSO, as well as through remote links with processes at high latitudes. Processes affecting the surface water heat budget of the oceans include advection, diffusion, net surface radiative flux, latent and sensible heat fluxes, and transfer of heat by precipitation (Curry and Webster, 1999). These fluxes maintain a balance as shown in Equation 1.

$$F^{net} - F^{adv} - F^{ent} = F^{rad} + F^{SH} + F^{LH} + F^{PR} \qquad \text{(Equation 1)}$$

Where the terms on the right hand side of the equation represent net radiative flux (F^{rad}), sensible and latent heat fluxes (F^{SH} and F^{LH}), and heat transfer due to precipitation (F^{PR}). These factors are balanced by the ocean heat storage term (F^{net}), advection (F^{adv}), and entrainment/diffusion (F^{ent}). While each of these terms plays a key role in determining the heat budget of a particular basin, this study will focus specifically on the role of advective processes in the determination of the equatorial Pacific heat budget.

In the tropical Pacific Ocean, the advective terms of Equation 1 can be quite large as a result of ENSO. Wyrtki (1985) analyzed data from the 1982-1983 El Niño event and determined that a transport of roughly 40 Sv (1 Sv = 1 x 10^6 m^3/s) occurred

from the western to the eastern Pacific during that event. Upon reaching the eastern coast, this water spread poleward, resulting in a net loss of heat at the equator (Wyrtki, 1985). Estimates of the eastward transport during the 1976 El Niño are smaller, yet substantial, at 27 Sv (Wyrtki, 1979). Also noted by Wyrtki is the build-up of warm water in the western warm pool prior to the 1976 and 1982 events. This warm water build up has been proposed as a mechanism, called the discharge – recharge paradigm, for the initiation of warm events (Jin, 1997).

Thermal constraints brought about by the depth of the thermocline in the equatorial Pacific are also of interest, as the shallow nature of the thermocline in the central and eastern portions of this basin allows for the development of unstable ENSO feedbacks. Prior to 3 Mya, advective processes did not play as large a role in climate variability in the equatorial Pacific. Since this time, however, shoaling of the thermocline in the eastern portion of this basin has caused the system to become much more sensitive to slight perturbations in advective fluxes (Philander and Fedorov, 2003). The transition from a deep to a shallow thermocline at 3 Mya may have resulted from surface ocean processes occurring at high latitudes (see e.g., Philander and Fedorov, 2003). Boccaletti et al. (2004) tested this hypothesis by performing calculations and model simulations with an imposed balanced heat budget at the surface of the oceans. They found that, with the balanced budget constraint, the depth of the thermocline at low latitudes could be controlled by the formation of deep water masses at high latitudes. During times of deep water formation, the ocean loses large amounts of heat at high latitudes, which is compensated by the shoaling of the thermocline at low latitudes and subsequent heat gain by the ocean. When deep water

formation is absent, there is less heat loss at high latitudes, a deeper thermocline in the low latitudes, and correspondingly less heat gain. The formation of deep water masses in the high latitudes and the zonal advection of momentum and heat along the equator are both important mechanisms influencing the equatorial Pacific heat budget. A third component of importance is the flow through the Indonesian Archipelago, typically referred to as the Indonesian throughflow.

1.4.2 Indonesian Throughflow

The geographic configuration along the western boundary of the Pacific is unique in the modern world oceans, as it allows for the transfer of water from the Pacific Ocean to the Indian Ocean via the Indonesian Seaways. Mean volume transports are estimated around 9 to 10 Sv (e.g., Gordon et al., 1999), with large seasonal and interannual variations (see e.g., Godfrey, 1996; Meyers, 1996; Murtugudde et al., 1998; Gordon et al., 1999; Potemra, 1999). The dominant pathway of water through the Indonesian Seas is shown in Figure 4. Low salinity water of the North Pacific is the primary source for flow through the Indonesian seas, occurring in the upper thermocline in the Makassar Strait (Gordon and Fine, 1996). Another component of throughflow in the deeper thermocline occurs along the eastern portion of the Indonesian Seas and originates from the more saline South Pacific (Gordon and Fine, 1996). The transport of water through the Indonesian Archipelago is an important component of the world's global thermohaline circulation (see e.g., Gordon, 1986). It also plays an important role in the heat budget

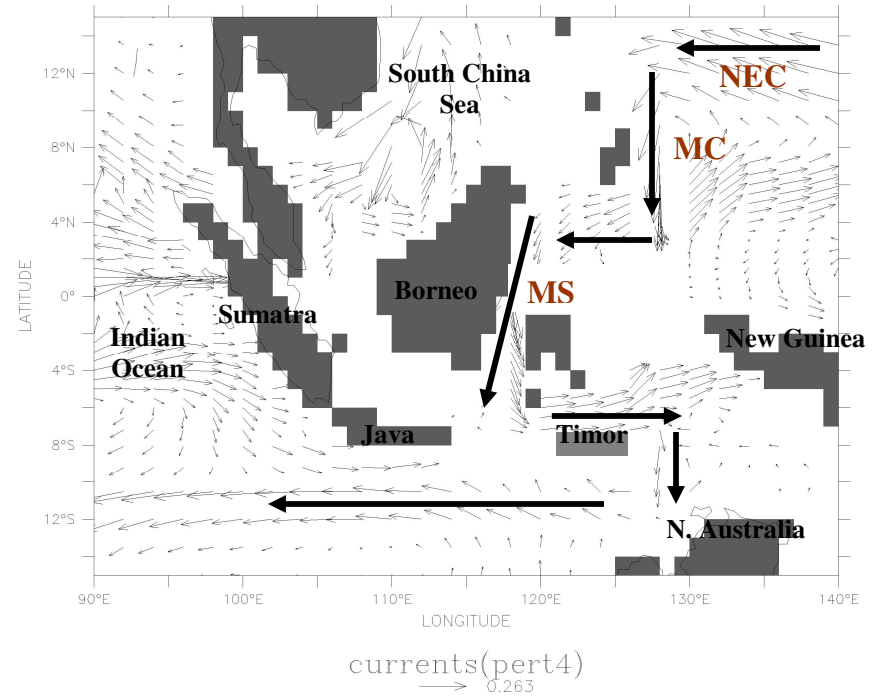

Figure 4. Map illustrating the dominant pathway through the Indonesian Archipelago. Water is fed to the Mindanao Current (MC) by the North Equatorial Current (NEC) and is then transported through the Makassar Strait (MS). It then passes around the eastern edge of Timor and travels west into the Indian Ocean.

of the equatorial Pacific and Indian Oceans, serving to warm the eastern Indian Ocean and cool the western Pacific (e.g., Hirst and Godfrey, 1993; Schneider, 1998; Murtugudde et al., 1998; Vranes et al., 2002).

Numerous studies have been completed to test the sensitivity of Indonesian throughflow (ITF) to geographic constraints and global circulation patterns. Early model studies by Hirst and Godfrey (1993) examined the impacts of an open versus closed ITF and established the importance of the throughflow as a thermal conveyor. Schneider (1998) expanded upon Hirst and Godfrey's work, showing that an open ITF leads to a westward shift of the western warm pool and convective region above, an acceleration of the equatorial undercurrent in the Pacific Ocean, and a deceleration in

the Indian Ocean. The geographic constraint of the latitudinal location of the ITF was tested by Rodgers et al. (2000). Their findings show that with the opening at 2˚N, the ITF is fed primarily by northern hemisphere water, the eastern Indian Ocean is warmer, the western Pacific Ocean is cooler, and the amplitude of the seasonal cycle is roughly 4.8 Sv. Conversely, with the opening of the ITF south of the equator at 3˚S, warmer water from the southern hemisphere dominantly feeds the ITF, and the amplitude of the seasonal cycle is much greater at 11 Sv. A subsequent study by Cane and Molnar (2001) also tested the affects of New Guinea's northward movement with model simulations and corroborated their results with paleoproxy data. They found that, as New Guinea drifted northward, the source water of the ITF came from the north, remotely impacting climate variability in eastern Africa. As previously noted, ITF is an important return flowpath for modern-day global thermohaline circulation. Shriver and Hurlburt (1997) determined that the presence of deep water formation in the North Atlantic enhances the ITF by 5.7 Sv and causes the throughflow to be more surface trapped.

1.4.3 Meridional Overturning Circulation and the ENSO

Timmermann et al. (2007) recently examined the role of meridional overturning circulation in the Atlantic Ocean on the ENSO. Using multiple, coupled model simulations, these researchers found that a substantial weakening in the overturning circulation in the North Atlantic, from 15-22 Sv to 2.5-6 Sv resulted in a strengthening of ENSO variability. This connection was noted to primarily occur via atmospheric feedbacks generated in the Atlantic Basin, which then impacted the strength of the seasonal cycle in the eastern Pacific Basin (Timmermann et al., 2007).

Conversely, an earlier study found that a shutdown of the overturning circulation in the Atlantic Basin resulted in a 10 to 40 meter deepening of the thermocline in the eastern portion of that basin and subsequent weakening in the amplitude of ENSO (Timmermann et al., 2005). It is apparent that an alteration of meridional overturning circulation does impact background climatology and ENSO, however the precise consequences on the strength and intensity of the ENSO remains in question.

The primary focus of recent studies has remained on the role of changes in overturning circulation in the Atlantic Basin. Deep water formation has been shown to occur in the Northern Pacific during past times of glaciation (see e.g., Gardner et al., 1982; Shackleton and Duplessy, 1985; Mammerickx, 1985; Corliss et al., 1986; Curry et al., 1988; Dean et al., 1989; Karlin et al., 1992; Lautenschlager et al., 1992; Lynch-Stieglitz and Fairbanks, 1994; Goldstein et al., 2000). This poses an interesting scenario, as a change in overturning circulation originating in the Pacific would occur more closely to the region where ENSO develops. Therefore, there is the potential to impact ENSO variability via global readjustments or via local responses within the Pacific Basin itself. In this study, it is hypothesized that intermediate water formation in the North Pacific will decrease the volume of Indonesian throughflow and warm the western warm pool of the tropical Pacific.

Chapter 2: METHODOLOGY

This climate study examines the impacts of a single, imposed perturbation on the circulation and thermal properties of the equatorial Pacific Ocean. Numerical simulations were used to achieve this goal. Model runs were completed using the Modular Ocean Model, version 4 (MOM4) developed at NOAA's Geophysical Fluid Dynamics Laboratory (GFDL) (Griffies et al., 2004). This is a primitive equation ocean model and is discretized on a fixed Eulerian grid. Both the control and perturbation runs were completed using a global domain. No variations in sea level were made; therefore the basin geometry is that of present day, with the exception of the Bering Strait, which was closed. The resolution was set to capture greater detail in the lower latitudes and more shallow waters. The horizontal resolution is 2º x 2º from 20ºN to 20ºS, telescoping to 2º x 4º poleward of these latitudes. Vertical resolution is 15 meters from the surface to 135 meters depth, transitions from 15 meters to 25 meters between 135 and 275 meters depth, and shifts from 25 meters to 1000 meters between 275 and 5000 meters depth. Levitus salinity and temperature (Levitus, 1982) and Hellerman wind stresses (Hellerman and Rosenstein, 1983) were used as the initial and boundary conditions for both runs. Two ocean-only simulations were completed using the computing facilities at GFDL in Princeton, New Jersey.

The control run was completed using the boundary conditions mentioned above. It was permitted to run for roughly 300 years. The last 5 years of the model output data were written and used as an equivalent for modern-day climatology. A second perturbation run was forced with an area of increased salinity of 3 PSU and

decreased temperature of 5ºC. The perturbation was centered at 50ºN and 170ºE and had a 6º gaussian width (see Figure 5). The perturbation simulation was run for roughly 700 years, with the last 5 years written as output. These data were treated as a new climatology for the system.

All analyses were completed using the graphical program Ferret. As this study examines the effects of a new climatological mean, all data used in the analyses were averaged over 2 years of the written output, unless otherwise noted. This removes any seasonal effects, which may be present.

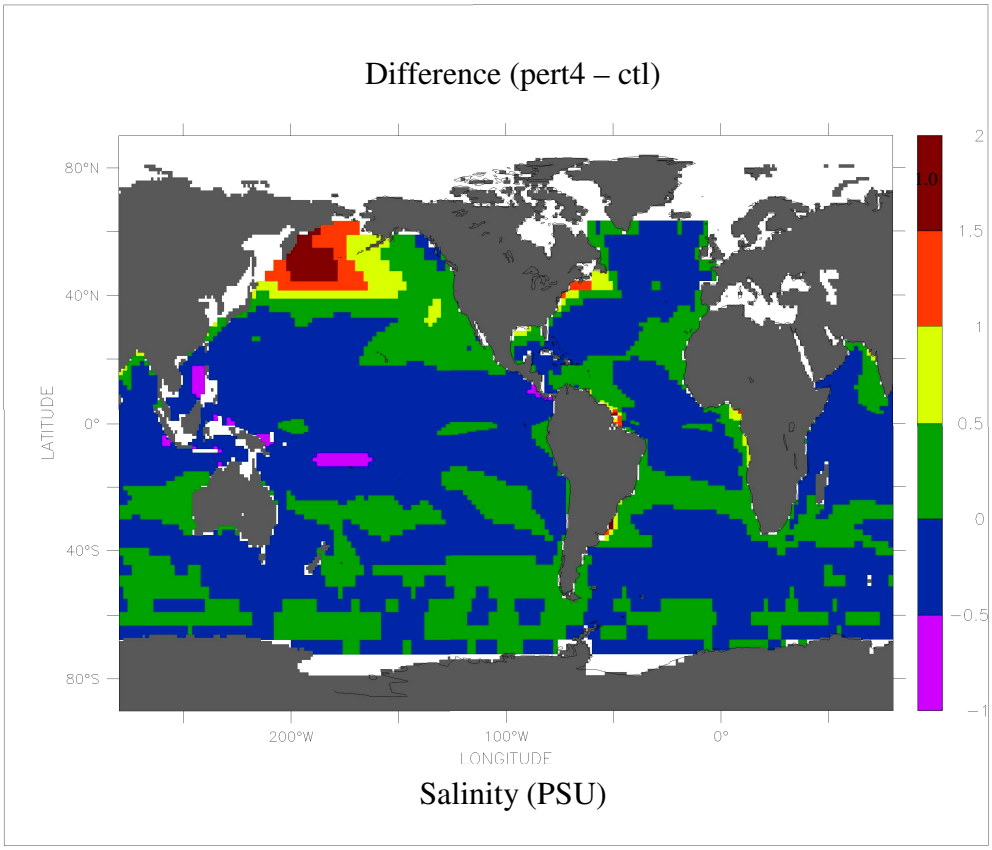

Figure 5. Plot of salinity difference between perturbation and control runs (given in PSU). Note the region of the imposed perturbation in the northern Pacific Ocean and the global domain of the model simulations. Regions of gray and white are not included in the ocean domain.

Chapter 3: RESULTS

3.1 Circulation Changes

3.1.1 Overturning Circulation

The imposed perturbation results in a change in the overturning circulation in the Northern Pacific Ocean when compared to the control run. Overturning circulation is reported as volume of flow (Sverdrup) averaged over the entire Pacific Basin. The control run simulates modern-day conditions, with no distinct southward flow originating from the northern Pacific (see Figure 6a). In the perturbation run, a southward flow is present with a volume of roughly 10 Sv (see Figure 6b). The difference in flow, as shown in Figure 6c, clearly illustrates an increase in southward flow of around 8 Sv centered at roughly 3000 meters and a corresponding increase in northward flow of the same magnitude focused at a depth of around 600 meters. While the imposed perturbation has generated a southward flow, this flow does not form a true deep water body, but instead forms an intermediate water mass. The perturbation also does not appear to penetrate across the equator into the southern portion of the basin.

3.1.2 Surface Currents

The structure of the surface currents within the northern Pacific basin remains roughly consistent between the control and perturbation runs, excluding some slight variations observed in the region of the imposed perturbation. This consistency of the overall current systems is expected given the imposed boundary conditions, as surface currents are primarily wind-driven, and modern climatological winds are used in both

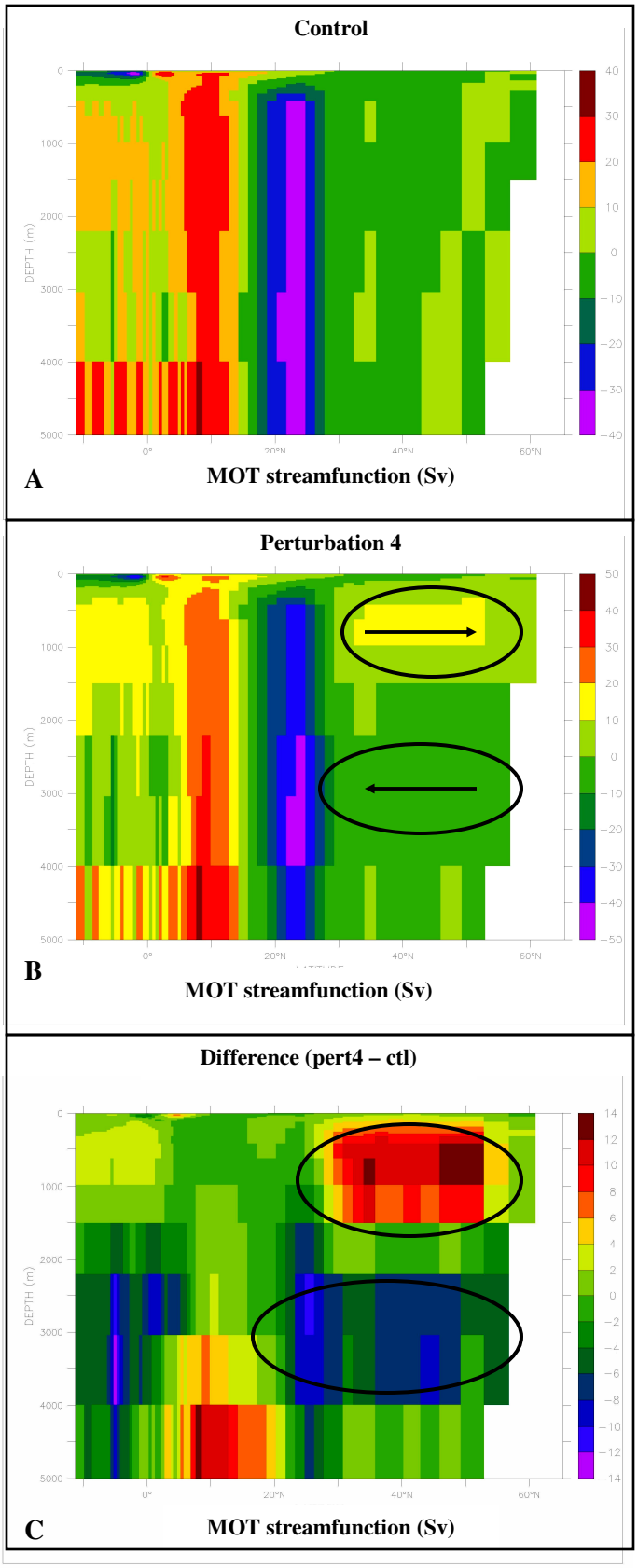

Figure 6. Plots of meridional overturning streamfunction integrated zonally across the Pacific Basin for the control run (A), perturbation run (B), and the difference between the perturbation and control runs (C). Negative values are indicative of southward transport. Units of transport are in Sverdrup. The control run lacks a region of organized southward flow out of the Northern Pacific. In the perturbation run, there is a region of southward flow originating from the North Pacific of roughly 10 Sv. The water mass is centered at approximately 3000 meters depth, and it is balanced by an increase in northward flow centered around 600 meters depth.

runs. Although the structure of the currents remains similar, the volume of flow does vary.

Of particular interest in this study is how the volume of water traveling through the Indonesian Seaways changes with the imposed high latitude perturbation. Measurements of ITF were calculated across the Makassar Strait at roughly 3ºS and were separated into the upper, lower, and full column flow. Table 1 shows the results of these calculations, with negative values reflecting southward flow. The total volume transport in the control run is 12.11 Sv, which is consistent with the modern day average of roughly 10 Sv (see Section 1.4.2). In the perturbation run, there is an overall annual decrease of 29% in the ITF. The same magnitude decrease is also observed in the monthly average transport values over one year of the model simulation (see Figure 7). The annually averaged flow values also show that the flow becomes more surface trapped, with the upper flow accounting for 68% of the overall flow in the perturbation run versus 60% in the control run. The decrease of 3.5 Sv in ITF corresponds well with an increased northward flow of roughly 2 Sv in the Kuroshio Current (see Figure 10).

	control (Sv)	**perturbation 4 (Sv)**	**Difference (Sv)**
Upper Layer (0-200m)	-7.3	-5.9	1.4
Lower Layer (200-1500m)	-4.8	-2.7	2.1
Full Column	-12.1	-8.6	3.5

Table 1. Volume of flow across Makassar Strait averaged over one year of the model output. All measurements are given in Sverdrup.

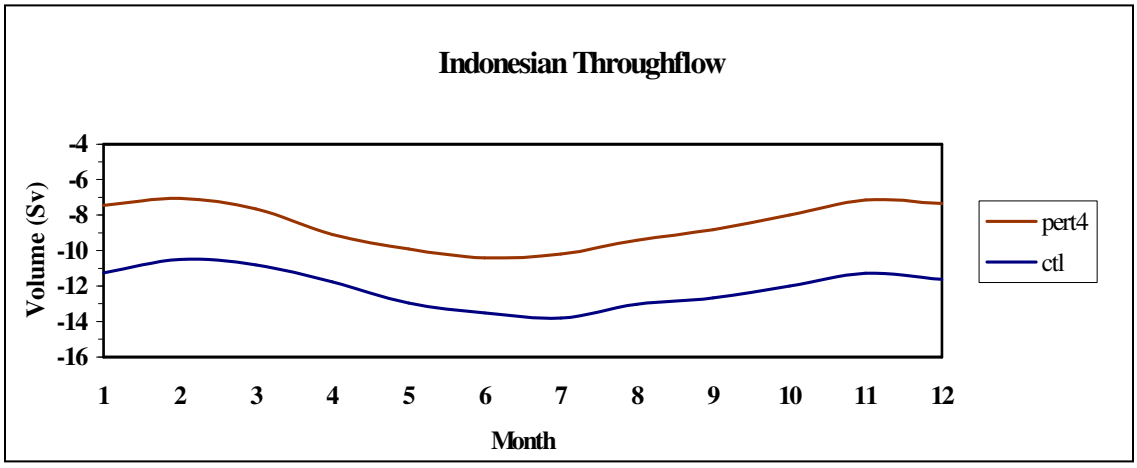

Figure 7. Monthly average of volume flow across Makassar Strait for the control and perturbation runs. The observed decrease in ITF of roughly 3.5 Sv occurs consistently in each month of the model simulation.

3.2 Thermal Structure of the Equatorial Pacific

3.2.1 Thermocline

The thermal structure of the equatorial Pacific is important to the development and behavior of ENSO. In the simulations of this study, the overall structure of the thermocline remains consistent with that of the modern day equatorial Pacific, with an upward tilt of the thermocline towards the eastern portion of the basin (see Figure 8). The imposed perturbation does, however, impact the temperature profile along the equatorial Pacific. A plot of temperature change averaged from 5ºS to 5ºN illustrates an overall warming in the surface water of the eastern and western region of the basin of up to 0.5ºC (see Figure 8). These regions of warming are only found in the upper 100 meters of the water column. Below 100 meters, there is an overall

cooling observed, with the strongest cooling of 1.25ºC centered at 300 meters in the western and central portion of the basin.

3.2.2 Sea Surface Temperatures

Sea surface temperature, as measured today, measures only the temperature of the surface water that is in contact with the atmosphere. These measurements are typically achieved remotely via satellite, but can also be obtained through in situ methods. While values in this study are reported as sea surface temperatures, they are, more accurately, the temperature of the upper model layer, which extends to a depth of 15 meters. Figure 9 shows the change in sea surface temperature between the perturbation and control runs. There is a large region of warming in the area of the western warm pool, with an average increase of 0.5ºC. There is a region of greater warming in the eastern portion of the basin, with increases of up to 1.5ºC. The remainder of the region along the equator sees a moderate cooling of 0.5ºC.

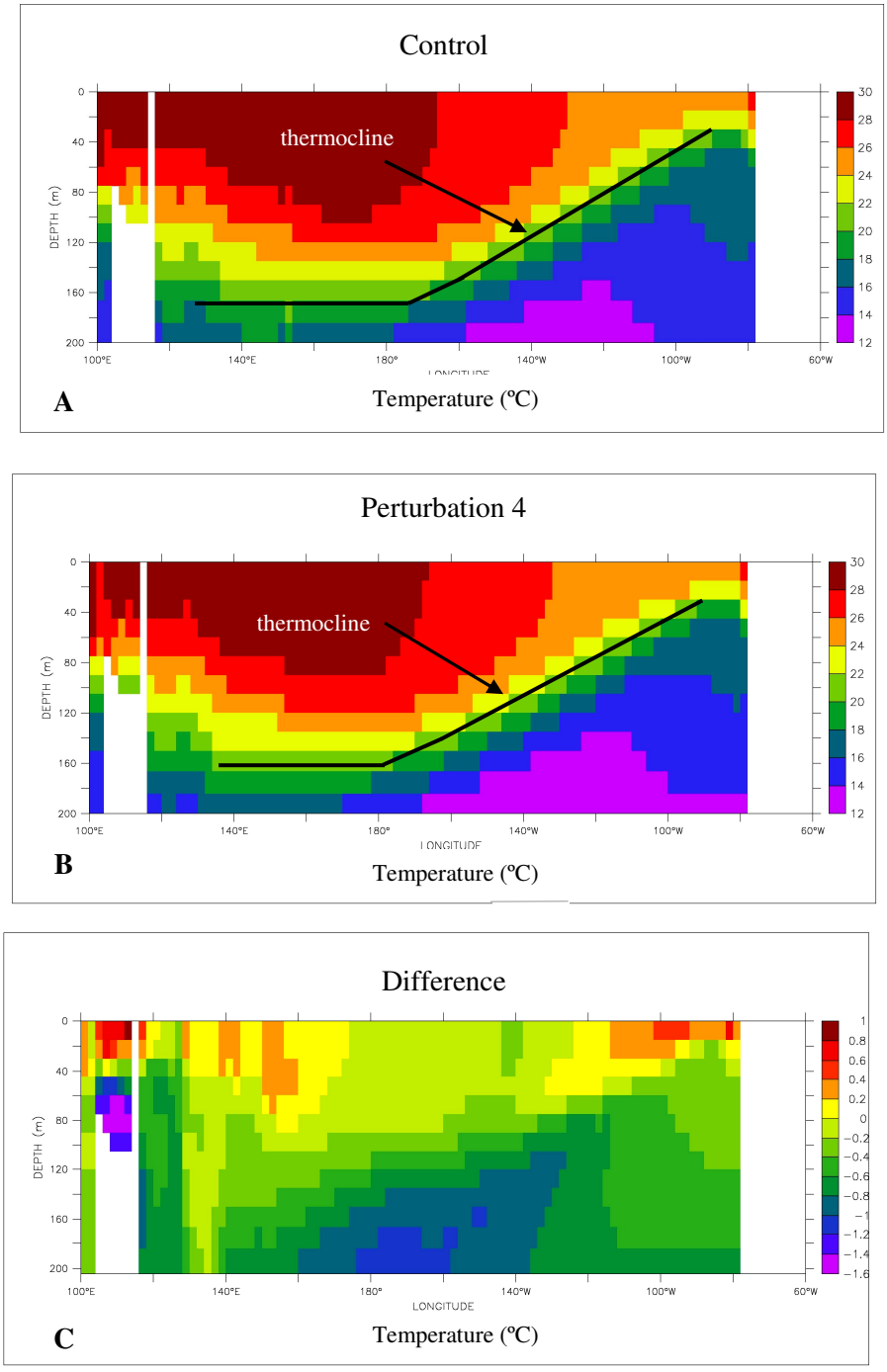

Figure 8. Plot of temperature across the equatorial Pacific Ocean for control run (A), perturbation run (B), and the difference between the perturbation and control runs (C). Values are averages over the NINO3 domain, from 5ºS to 5ºN. All potential temperature values are given as ºC. Even though there is no overall change in the structure of the thermocline between the control and perturbation runs, there is warming of up to 0.5ºC in the upper 40 meters in the western and eastern Pacific.

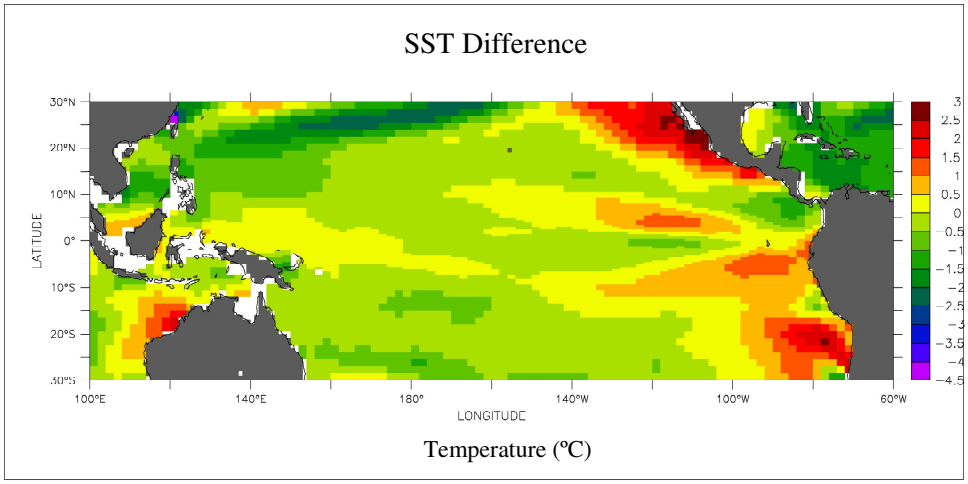

Figure 9. Plot of sea surface temperature difference in the tropical Pacific Basin. The simulation of an intermediate body of water flowing out of the northern Pacific results in a warming of roughly 0.5ºC in the western tropical Pacific. In the eastern tropical Pacific sea surface temperatures increase up to 1.5ºC. Given a fully coupled system, these temperature anomalies could lead to either more permanent El Niño-like conditions or more intense/frequent ENSO events.

Chapter 4: DISCUSSION

4.1 The Role of NPIW on Circulation in the Northern Pacific Basin

The formation of an intermediate water mass in the Northern Pacific Ocean results in a noticeable decrease in the volume of flow through the Indonesian Seaways. Links between the high latitude perturbation and low latitude response occur primarily as changes in volume of flow in the existing surface current system. However, slight changes in the structure of flow near the location of the imposed perturbation are also proposed as a potential mechanism linking the two regions. The observed intermediate water body of roughly 10 Sv that is generated in the perturbation run travels southward from the Northern Pacific at approximately 3000 meters depth. Due to the conservation of mass, an approximately equal volume of water is then pulled northward at shallower depths to compensate for the sinking water in the north. It is this increase in the northward flow, primarily occurring along the western boundary, which links the sinking water in the north with the decrease in ITF found in the tropics.

The pathways feeding into the ITF are shown in Figure 10. Water moves from the eastern to the western tropical Pacific along the north equatorial current (NEC). Once reaching the western boundary, the water splits into northward and southward components. The southward flow travels along the Mindanao Current (MC), which branches to the east as a return flow in the north equatorial counter current (NECC). The Mindanao Current also branches to the west, feeding the ITF. When the NEC reaches the western edge of the basin, the northward limb feeds into the western boundary Kuroshio Current. The northward transport along the Kuroshio

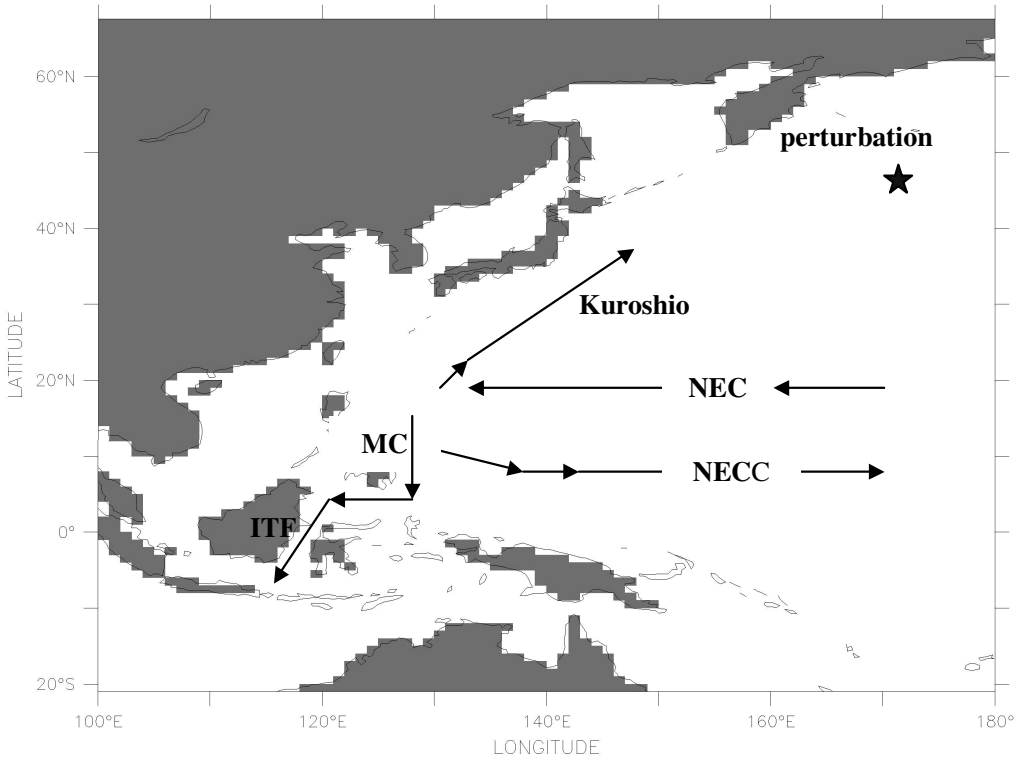

Figure 10. Map illustrating the general pathways of flow along the western equatorial Pacific. When the North Equatorial Current (NEC) reaches the western boundary, it branches to the north as the Kuroshio Current and to the south as the Mindanao Current (MC). Part of the Mindanao Current returns to the east as the North Equatorial Counter Current (NECC), while the remainder feeds the Indonesian Througflow (ITF). In the simulations of this study, water was pirated from the Mindanao Current, and ultimately the ITF, to feed into the perturbation region of the northern Pacific via the Kuroshio Current.

Current increases 2 Sv in the perturbation run, helping to feed the sinking intermediate water mass in the higher latitudes. A consequence of this increase in northward flow along the Kuroshio is a decrease in the volume of flow heading southward from the western edge of the NEC. This decrease in flow is primarily accounted for as the observed decrease in the ITF, as the volume of the NECC remains the same between the control and perturbation runs.

Given the constraints of this study, the observed 29% decrease in ITF is considered to be significant. Additional responses within the climate system during periods of large-scale glaciations that are not accounted for in this study, such as shifts in atmospheric convection, changes in basin geometry, and altered strength of the seasonal cycle could further impact the ITF by either amplifying the simulated decrease in flow or by serving to damp the observed effects. These possibilities raise even more questions as to how the background climatology during cold climatic regimes may have impacted ITF and, hence, ENSO. Section 4.4 discusses what types of future studies are suggested to further investigate this link.

While altered volume of flow in the surface currents is one mechanism linking the high latitude perturbation with the low latitude climatology, another aspect of circulation change that is of particular interest is the role on shallow meridional overturning (MOT) cells. These cells are believed to circulate on decadal timescales, transmitting mid-latitude sea surface temperature perturbations southward to the equator, where they upwell, couple with the atmosphere, and impact ENSO variability (Gu and Philander, 1997). For this study, the decadal nature and precise structure of the cells are not in question, but rather if the cells have seen an overall increase or decrease in flow. A calculation of the volume of southward flow integrated from 300 to 500 meters depth across 20ºN shows an increase of roughly 1.3 Sv in the perturbation run. Examination of a temperature difference plot averaged over the central and western Pacific reveals the presence of a temperature anomaly closely resembling the structure of these shallow MOT cells (see Figure 11). A warming of 2ºC originates at the surface around 40ºN and continues at 600 meters

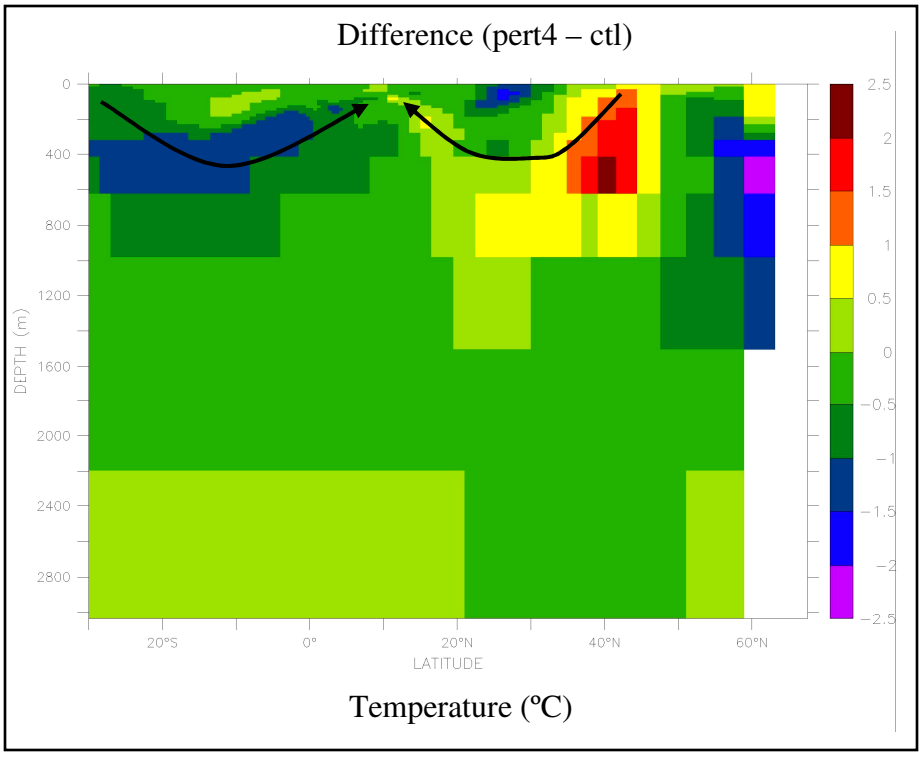

Figure 11. Meridional temperature difference averaged from 160ºE to 200ºE. Note the region of warming extending from 45ºN toward the equator. Arrows indicate the proposed structure of shallow Meridional Overturning (MOT) Cells (Langenberg, 2002). The southward transport of a warm surface temperature anomaly via MOT cells is one potential mechanism accounting for the warmer SSTs in the tropical Pacific of the perturbation run.

depth until approaching the surface near the equator. The region of warming diminishes from 2ºC to 0.5ºC as it approaches the equator. The origin of the observed warm anomaly in the surface water at 40ºN is likely a result of minor variations in the structure of the surface currents in that region. Figure 12 shows the surface currents in the control and perturbation runs and temperature of the surface water. The control run shows the modern-day current structure, with cyclonic circulation beneath the subpolar low and anticyclonic circulation beneath the subtropical high. This drives the northward flow of warm water along the Kuroshio Current and southward flow of

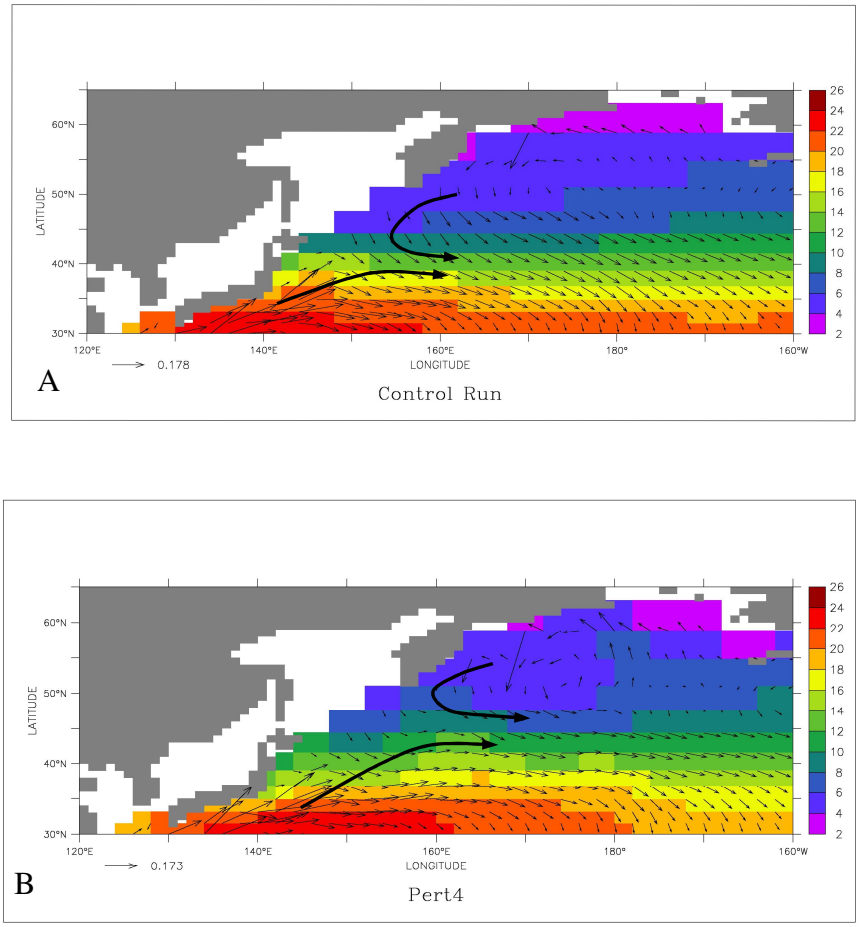

Figure 12. Plot of surface currents for month 12 (vectors) over sea surface temperature (shaded) for control run (A) and perturbation run (B) in the Northwestern Pacific. Darker arrows indicate the general location of the northward flowing Kuroshio Current and the southward flowing Oyashio Current, which intersect along the subpolar front. As a result of the imposed perturbation, there is a northward shift in the subpolar front in the perturbation run. This shift leads to a warm water anomaly centered around 45ºN and 160ºE (see Figure 13).

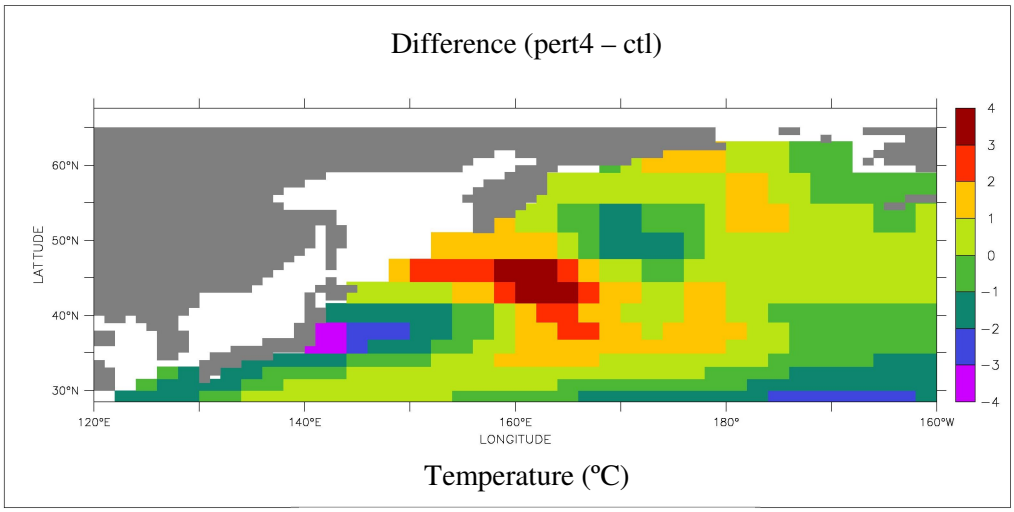

Figure 13. Plot of sea surface temperature difference between the perturbation and control runs. Note the warm water anomaly of roughly 4ºC centered at 45ºN. This is the proposed source region of warm water corresponding to the warm anomaly shown in Figure 11.

cool water along the Oyashio Currrent. These two currents intersect around 40ºN and move eastward in a region that is referred to as the subpolar front. In the perturbation run, there is an observed shift in circulation in this region, with warmer water from the Kuroshio Current being pulled northward into the region of the imposed perturbation (see Figures 12 and 13). The combined effects of decreasing the ITF and the potential increase in supply of subtropical surface water are to warm the surface water in the equatorial Pacific Ocean.

4.2 Implications of Thermal Variations on the ENSO

As hypothesized, the observed decrease in ITF results in a warming of the western tropical Pacific. This is due to the decrease in advective flux of warm water from the western Pacific to the eastern Indian Ocean via the ITF. Figure 14 illustrates the corresponding cooling observed in the surface water of the eastern Indian Ocean. The surface temperatures and thermocline structure in the eastern Pacific basin are

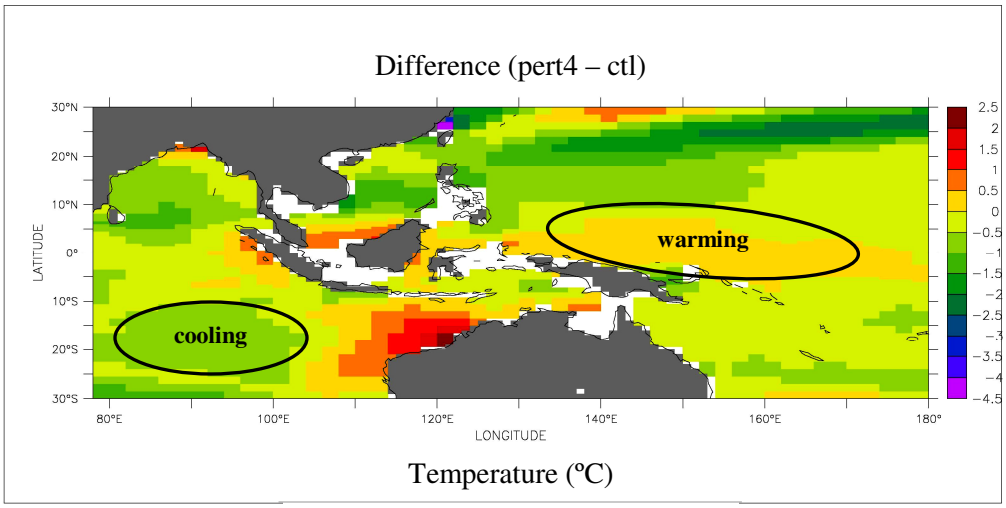

Figure 14. Plot of sea surface temperature difference between the perturbation and controls runs. Decreased volume of ITF in the perturbation run leads to a cooling of 1ºC in the eastern Indian Ocean and a warming of 0.5ºC in the western Pacific Ocean.

largely determined by surface wind forcing. The tradewinds in this region drive coastal upwelling, pulling the cooler water toward the surface. The maintenance of the overall structure of the thermocline across the equatorial Pacific is consistent with the modern-day surface wind forcing used in both the control and perturbation runs. Since the imposed anomaly in the northern Pacific does not penetrate into the southern basin, there is no reorganization of the global thermohaline circulation which, as discussed in Section 1.3.2 is one potential mechanism controlling thermocline depth in the lower latitudes.

Even though the impacts of the imposed perturbation are local, there is still a significant response in the thermal structure of the surface waters of the equatorial Pacific. The observed warming in the western and eastern portions of the basin reaches values of 0.5 to 1.5ºC, respectively (see Figure 9). Values such as these are

considered to be significant, since warming during a typical El Niño ranges from 1 to 4ºC, with an average around 2ºC. The distribution, however, of the warmer water along the equator does not resemble that of an ENSO event. This is most likely due to the continued surface wind forcing of modern-day conditions. These winds continue to drive coastal upwelling, pushing cool water westward along the equator. The accumulation of warm water occurring in the western equatorial Pacific is partially being stored in the western warm pool. The remainder is advecting eastward, where it is partially transported poleward along the coast as coastal Kelvin waves and partially being carried back toward the center of the basin via Rossby waves. These mechanisms of transport, along with the surface wind forcing, could explain the asymmetric pattern of sea surface temperature anomalies observed in Figure 9.

The changes in climatology observed in the equatorial Pacific of the perturbation run could impact the development and periodicity of ENSO. This study only examined the changes within the ocean basin of the imposed perturbation. However, given the warming seen in the western and eastern tropical Pacific, conditions are favorable for the development of either more permanent El Niño-like conditions or more frequent/intense ENSO events. It is proposed that, if coupled with an atmospheric model, the resultant oceanic warming could permit the shifting of atmospheric convection toward the center of the basin. The concept of zonal distribution of coupling strength proposed by Suarez and Schopf (1988) is one mechanism by which the original perturbation could grow, if allowed to penetrate into the central basin. As the ITF decreased and warming of the western basin

increased, the western warm pool would move toward the east, taking with it the corresponding region of convection. As the perturbation reached the central basin, the coupling strength would grow, making the effects even greater. The anomalous surface winds would decrease the southeasterly tradewinds, feeding back on the initial perturbation in a positive fashion. Given a sustained decrease in ITF and supply of warm water, these mechanisms could produce new, stable conditions where the thermocline is "permanently" suppressed in the eastern equatorial Pacific. This would be analogous to more permanent El Niño-like conditions.

A second adjustment of the system to the decrease in ITF could be more intense and frequent ENSO events. As discussed in Section 1.4.1, there has been an observed build up of warm water in the western warm pool associated with the discharge-recharge hypothesis for ENSO development. The observed decrease in ITF in this study could provide additional warm water in the western warm pool, or a "build up of warm water" necessary to initiate an ENSO event. Since the water would likely accumulate more quickly, conditions could possibly become more favorable for El Niño to occur more frequently. If ENSO events did not occur more frequently, they would likely be more intense, as the volume of warm water available to advect eastward would be greater.

4.3 Conclusions

The numerical simulations completed for this study are a first step at examining the role, if any, that a Northern Pacific sinking water mass may play in ENSO variability, as is hypothesized to have occurred during times of large-scale glaciations in the past. The results of this study demonstrate the significance of the

response in the Pacific Basin to the imposed intermediate water formation. First, there is a notable decrease of 29% in the volume of water passing through the Indonesian Seaway, resulting in the warming of the western and eastern tropical Pacific surface water. This observed warming provides conditions favorable for a more permanent El Niño – like climatology or, possibly more intense or frequent ENSO events (see Figure 15 for a summary of proposed mechanisms leading to warmer SSTs in tropical Pacific). Second, the imposed perturbation is not large enough to interrupt the existing global thermohaline conveyor. As such, the water mass remains at an intermediate depth and does not pass south of the equator. This is a significant point, as it reveals that local variations in circulation of the Northern Hemisphere Pacific can substantially impact the tropics and ENSO variability. In conclusion, it is important to acknowledge the full complexity of the climate system. The role of multiple, coupled systems creates many challenging questions for scientists to unravel. With each progressing year, new advances are made, solving some problems and creating new ones as well.

4.4 Suggestions for Future Work

Suggestions for future work initially include a coupled run on the Cane-Zebiak Model using the new climatological sea surface temperatures from this study. The CZ model is a limited domain model and is computationally inexpensive. This would provide a first order approximation of how the ENSO system would respond in a more realistic coupled setting. Given future opportunity and resources, a fully coupled global simulation (ocean-atmosphere) would be recommended. Several experiments could be fruitful. First, a global coupled run given only the perturbations

used in this study. This would show whether or not the imposed perturbation would impact the existing global thermohaline circulation, and it could also provide more insight as to ENSO variability, since the atmosphere would actively respond to changes in the ocean. Second, a global coupled run altered to include a lower sea level of the magnitude that occurs during large-scale glaciations. Since the Indonesian Seaway is rather shallow and narrow, changes in sea level could potentially have a large impact on the geometry of the coastline and volume of ITF. Finally, making alterations to deep water formation throughout the world would also be insightful, such as decreasing or stopping North Atlantic Deep Water, while increasing North Pacific Deep Water.

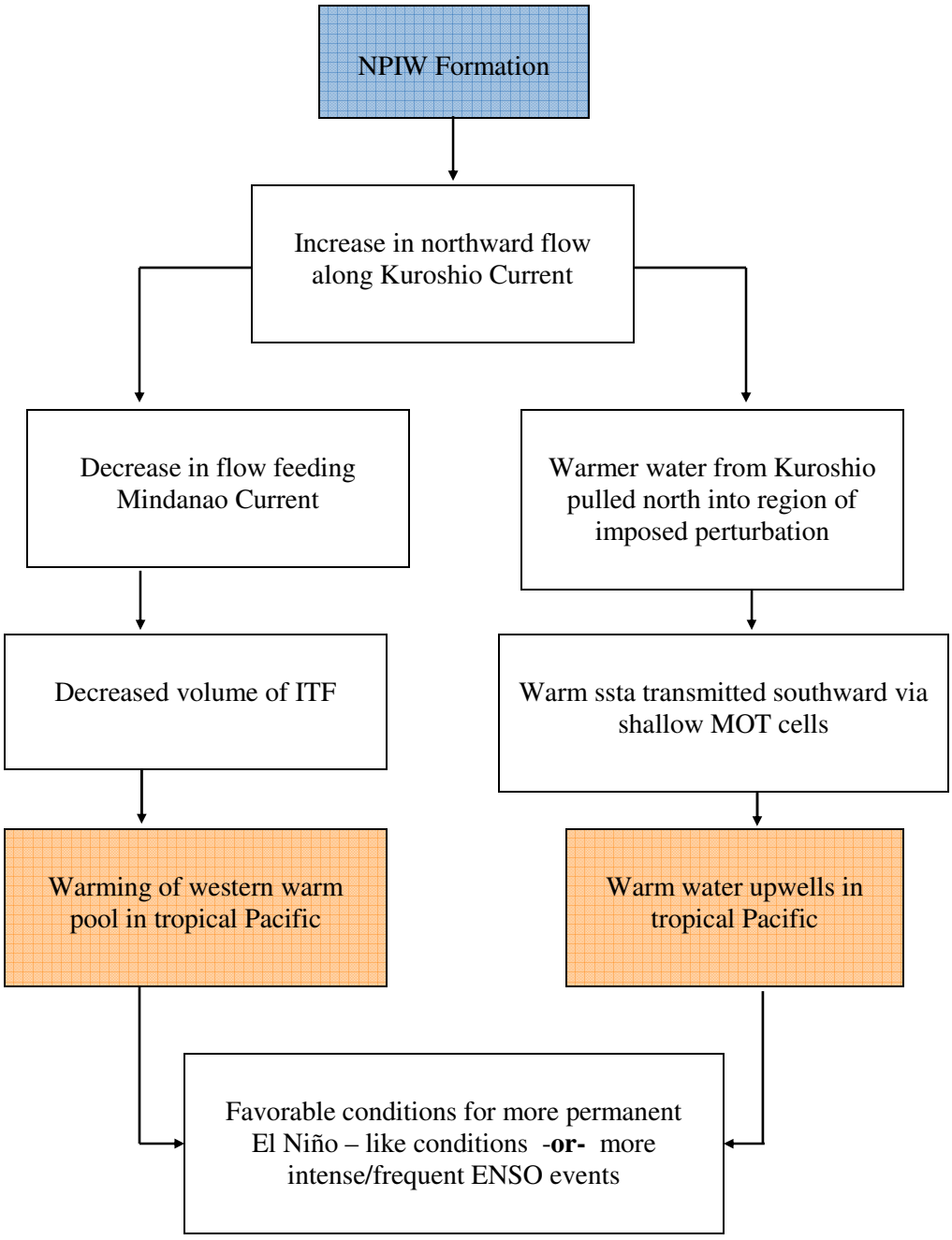

Figure 15. Flow-chart illustrating two possible mechanisms linking the imposed high latitude perturbation with the observed low latitude response. In both scenarios the formation of NPIW results in a strengthening of the northward flowing Kuroshio Current, which causes a decrease in ITF and northward shift of the subpolar front. These changes lead to the build up of warm water in the equatorial Pacific and create conditions favorable for a more persistent El Niño – like climatology.

Bibliography

Andreasen, D. J., Ravelo, A. C. Tropical Pacific Ocean Thermocline Depth Reconstructions for the Last Glacial Maximum. *Paleoceanography*, **12**, No. 3, pp. 395-413, (1997).

Berger, A. L. Long – Term Variations of Daily Insolation and Quaternary Climatic Changes. *Journal of the Atmospheric Sciences*, **35**, pp. 2362-2367, (1979).

Bjerknes, J. Atmospheric Teleconnections from the Equatorial Pacific. *Monthly Weather Review*, **97**, No. 3, pp. 163-172, (1969).

Boccaletti, G., Pacanowski, R. C., Philander, S. G. H., Fedorov, A. V. The Thermal Structure of the Upper Ocean. *Journal of Physical Oceanography*, **34**, pp. 888-902, (2004).

Cane, M. A., Molnar, P. Closing of the Indonesian Seaway as a Precursor to East African Aridification Around 3-4 Million Years Ago. *Nature*, **411**, pp. 157-162, (2001).

Clement, A. C., Seager, R., Cane, M. A. Suppression of El Niño During the Mid-Holocene by Changes in the Earth's Orbit. *Paleoceanography*, **15**, No. 6, pp. 731-737, (2000).

Clement, A. C., Seager, R. Cane, M. A. Orbital Controls on the El Niño/Southern Oscillation and the Tropical Climate. *Paleoceanography*, **14**, No. 4, pp. 441-456, (1999).

Corliss, B. H., Martinson, D. G, Keffer, T. Late Quaternary Deep-Ocean Circulation. *Geological Society of America Bulletin*, **97**, pp. 1106-1121, (1986).

Curry, J. A., Webster, P. J. Thermodynamics of Atmospheres and Oceans. Academic Press, (1999).

Curry, W. B., Duplessy, J. C., Labeyrie, L. D., Shackleton, N. J. Changes in the Distribution of $\delta^{13}C$ of Deep Water $\sum CO_2$ Between the Last Glaciation and the Holocene. *Paleoceanography*, **3**, No. 3, pp. 317-341, (1988).

Dean, W. E., Gardner, J. V., Hemphill-Haley, E. Changes in Redox Conditions in Deep- Sea Sediments of the Subarctic North Pacific Ocean: Possible Evidence for the Presence of North Pacific Deep Water. *Paleoceanography*, **4**, No. 6, pp. 639-653, (1989).

Gardner, J. V., Dean, W. E., Klise, D. H., Baldauf, J. G. A Climate-Related Oxidizing Event in the Deep-Sea Sediment from the Bering Sea. *Quaternary Research*, **18**, pp. 91-107, (1982).

Godfrey, J. S. The Effect of the Indonesian Throughflow on Ocean Circulation and Heat Exchange with the Atmosphere: A Review. *Journal of Geophysical Research*, **101**, No. C5, pp. 12217-12237, (1996).

Goldstein, S. L., Hemming, S. R., Piotrowski, A. M., Machlus, M. North Pacific Deep Water Formation During the Last Glacial Maximum? *Goldschmidt Conference Journal of Conference Abstracts*, Goldschmidt, Oxford, UK, **5(2)**, pp. 448, (2000).

Gordon, A. L., Dwi Susanto, R., Ffield, A. Throughflow within Makassar Strait. *Geophysical Research Letters*, **26**, No. 21, pp. 3325-3328, (1999).

Gordon, A. L., Fine, R. A. Pathways of Water Between the Pacific and Indian Oceans in the Indonesian Seas. *Nature*, **379**, pp. 146-149, (1996).

Gordon, A. L. Interocean Exchange of Thermocline Water. *Journal of Geophysical Research*, **91**, No. C4, pp. 5037-5046, (1986).

Griffies, S. M., Harrison, M. J., Pacanowski, R. C., Rosati, A. A Technical Guide to MOM4 GFDL Ocean Group Technical Report No.5. NOAA / Geophysical Fluid Dynamics Laboratory, available online at www.gfdl.noaa.gov, (2004).

Gu, D., Philander, S. G. H. Interdecadal Climate Fluctuations That Depend on Exchanges Between the Tropics and Extratropics. *Science*, **275**, pp. 805-807 (1997).

Gurney, R. J., Foster, J. L., Parkinson, C. L. Editors Atlas of Satellite Observations Related to Global Change. Cambridge University Press, (1993).

Hays, J. D., Imbrie, J., Shackleton, N. J. Variations in the Earth's Orbit: Pacemaker of the Ice Ages. *Science*, **194**, No. 4270, pp. 1121-1132, (1976).

Hellerman, S., Rosenstein, M. Normal Monthly Stress Over the World Ocean with Error Estimates. *Journal of Physical Oceanography*, **13**, pp. 1093-1104, (1983).

Hirst, A. C., Godfrey, J. S. The Role of Indonesian Throughflow in a Global Ocean GCM. *Journal of Physical Oceanography*, **23**, pp. 1057-1086, (1993).

Jin F.F. An Equatorial Ocean Recharge Paradigm for ENSO. Part I: Conceptual Model. *Journal of Atmospheric Sciences*, **54**, pp. 811-829, (1997).

Karlin, R., Lyle, M., Zahn, R. Carbonate Variations in the Northeast Pacific During the Late Quaternary. *Paleoceanography*, **7**, No. 1, pp. 43-61, (1992).

Koutavas, A., Lynch-Stieglitz, J., Marchitto Jr., T. M., Sachs, J. P. El Niño – Like Pattern in Ice Age Tropical Pacific Sea Surface Temperature. *Science*, **297**, pp. 226-230, (2002).

Kukla, G. J., Clement, A. C., Cane, M. A., Gavin, J. E., Zebiak, S. E. Last Interglacial and Early Glacial ENSO. *Quaternary Research*, **58**, pp. 27-31, (2002).

Langenberg, H., A Slower Flow. *Nature*, **415**, pp. 594, (2002).

Latif, M., Barnett, T. P. Causes of Decadal Climate Variability Over the North Pacific and North America. *Science*, **266**, pp. 634-637, (1994).

Lautenschlager, M., Mikolajewicz, U., Maier-Reimer, E., Heinze, C. Application of Ocean Models For the Interpretation of Atmospheric General Circulation Model Experiments on the Climate of the Last Glacial Maximum. *Paleoceanography*, **7**, No. 6, pp. 769-782, (1992).

Lea, D. W., Pak, D. K., Spero, H. J. Climate Impact of Late Quaternary Equatorial Pacific Sea Surface Temperature Variations. *Science*, **289**, pp. 1719-1924, (2000).

Levitus, S. Climatological Atlas of the World Ocean. *NOAA Prof. Pap. 13*, pp. 173, U.S. Government Printing Office, Washington, D.C., (1982).

Liu, Z., Herbert, T. D. High-Latitude Influence on the Eastern Equatorial Pacific Climate in the Early Pleistocene Epoch. *Nature*, **427**, pp. 720-723, (2004).

Lynch-Stieglitz, J., Fairbanks, R. G. A Conservative Tracer for Glacial Ocean Circulation from Carbon Isotope and Palaeonutrient Measurements in Benthic Foraminifera. *Nature*, **369**, pp. 308-310, (1994).

Mammerickx, J. A Deep-Sea Thermohaline Flow Path in the Northwest Pacific. *Marine Geology*, **65**, pp. 1-19, (1985).

McPhaden, J. M., Busalacchi, A. J., Cheney, R., Donguy, J.-R., Gage, K. S., Halpern, D., Ji, M., Julian, P., Meyers, G., Mitchum, G. T., Niiler, P. P., Picaut, J., Reynolds, R. W., Smith, N., Takeuchi, K., The Tropical Ocean-Global Atmosphere Observing System: A Decade of Progress. *Journal of Geophysical Research*, **103**, No. C7, pp. 14169-14240 (1998).

Meyers, G. Variation of Indonesian Throughflow and the El Niño – Southern Oscillation. *Journal of Geophysical Research*, **101**, No. C5, pp. 12255-12263, (1996).

Milankovitch, M. M. Canon of insolation and the ice age problem. Koniglich Serbische Akademie, Beograd. Translation, *Israel Prog. Sci. Trans*., Washington D. C. (1941).

Murtugudde, R., Busalacchi, A. J., Beauchamp, J. Seasonal-to-Interannual Effects of the Indonesian Throughflow on the Tropical Indo-Pacific Basin. *Journal of Geophysical Research*, **103**, No. C10, pp. 21425-21441, (1998).

Philander, S. G., Fedorov, A. V. Role of Tropics in Changing the Response to Milankovich Forcing Some Three Million Years Ago. *Paleoceanography*, **18**, No. 2, 1045, doi:10.1029/2002PA000837, (2003).

Philander, S. G. El Niño, La Niña, and the Southern Oscillation. Academic Press, Inc., (1990).

Philander, S. G. H., Yamagata, T., Pacanowski, R. C., Unstable Air-Sea Interactions in the Tropics. *Journal of the Atmospheric Sciences*, **41**, No. 4, pp. 604-613, (1984).

Picaut, J., Hackert, E., Busalacchi, A. J., Murtugudde, R., Lagerloef, G. S. E. Mechanisms of the 1997-1998 El Niño – La Niña, as Inferred from Space-Based Observations. *Journal of Geophysical Research*, **107**, No. C5, 10.1029/2001JC000850, (2002).

Potemra, J. T. Seasonal Variations of Upper Ocean Transport from the Pacific to the Indian Ocean via Indonesian Straits. *Journal of Physical Oceanography*, **29**, pp. 2930-2944, (1999).

Rasmusson, E. M., Carpenter, T. H. Variations in Tropical Sea Surface Temperature and Surface Wind Fields Associated with the Southern Oscillation/El Niño. *Monthly Weather Review*, **110**, pp. 354-384, (1982).

Rodbell, D. T., Seltzer, G. O., Anderson, D. M., Abbott, M. B., Enfield, D. B., Newman, J. H. An ~15,000-Year Record of El Niño-Driven Alluviation in Southwestern Ecuador. *Science*, **283**, pp. 516-520, (1999).

Rodgers, K. B., Latif, M., Legutke, S. Sensitivity of Equatorial Pacific and Indian Ocean Watermasses to the Position of the Indonesian Throughflow. *Geophysical Research Letters*, **27**, No. 18, pp. 2941-2944, (2000).

Schneider, N., Miller, A. J., Alexander, M. A., Deser, C. Subduction of Decadal North Pacific Temperature Anomalies: Observations and Dynamics. *Journal of Physical Oceanography*, **29**, pp. 1056-1070, (1999).

Schneider, N. The Indonesian Throughflow and the Global Climate System. *Journal of Climate*, **11**, pp. 676-689, (1998).

Shackleton, N. J., Duplessy, J. –C. Carbon Isotope Evidence for Formation of North Pacific Deep Water at 18 ka BP Glacial Maximum. *Eos*, **66**, No. 18, pp. 292, (1985).

Shriver, J. F., Hurlburt, H. E. The Contribution of the Global Thermohaline Circulation to the Pacific to Indian Ocean Throughflow via Indonesia. *Journal of Geophysical Research*, **102**, No. C3, pp. 5491-5511, (1997).

Stott, L., Poulsen, C., Lund, S., Thunell, R. Super ENSO and Global Climate Oscillations at Millennial Time Scales. *Science*, **297**, pp. 222-226, (2002).

Suarez, M. J., Schopf, P. S. A Delayed Action Oscillator for ENSO. *Journal of the Atmospheric Sciences*, **45**, No. 21, pp. 3283-3287, (1988).

Timmerman, A., Okumura, Y., An, S.-I., Clement, A., Dong, B., Guilyardi, E., Hu, A., Jungclaus, J. H., Renold, M., Stocker, T. F., Stouffer, R. J., Sutton, R., Xie, S.-P., Yin, J. The Influence of a Weakening of the Atlantic Meridional Overturning Circulation on ENSO. *Journal of Climate*, **20**, pp. 4899-4919 (2007).

Timmerman, A., An, S., Krebs, U., Goosse, H. ENSO Suppression Due to Weakening of the North Atlantic Thermohaline Circulation. *Journal of Climate*. **18**, pp. 3122-3139 (2005).

TOGA Special Issue of JGR-Oceans. *Journal of Geophysical Research*, **103**, No. C7, (1998).

Tudhope, A. W., Chilcott, C. P., McCulloch, M. T., Cook, E. R., Chappell, J., Ellam, R. M., Lea, D. W., Lough, J. M., Shimmield, G. B. Variability in the El Niño-Southern Oscillation Through a Glacial Interglacial Cycle. *Science*, **291**, pp. 1511-1517 (2001).

Vranes, K., Gordon, A. L., Ffield, A. The Heat Transport of the Indonesian Throughflow and Implications for the Indian Ocean Heat Budget. *Deep-Sea Research II*, **49**, pp. 1391-1410, (2002).

Wyrtki, K. Water Displacements in the Pacific and the Genesis of El Niño Cycles. *Journal of Geophysical Research*, **90**, No. C4, pp. 7129-7132, (1985).

Wyrtki, K. The Response of Sea Surface Topography to the 1976 El Niño. *Journal of Physical Oceanography*, **9**, pp. 1223-1231, (1979).

Zebiak, S. E., Cane, M. A. A Model El Niño-Southern Oscillation. *Monthly Weather Review*, **115**, pp. 2262-2278, (1987).

Zhang, R.-H., Rothstein, L. M., Busalacchi, A. J. Origin of Upper-Ocean Warming and El Niño Change on Decadal Scales in the Tropical Pacific Ocean. *Nature*, **391**, pp. 879-883, (1998).